The Impact of Substitution of Diphenyl Dialumene on the Molecular Structure and Energetic Properties

Salma Babikir[1], Sahar Abdalla[2,3*], Wefag Mohamed[1], and Yunusa Umar[4]

[1]*Department of Chemistry, Faculty of Education, Khartoum University, Khartoum 11115, Sudan*

[2]*Department of Chemistry, College of Science, Imam Mohammad Ibn Saud Islamic University (IMSIU), Riyadh 11623, Saudi Arabia*

[3]*Department of Chemistry, Faculty of Science, Khartoum University, Khartoum 11115, Sudan*

[4]*Department of Chemical Engineering, Jubail Industrial College, Jubail Industrial City, Jubail 31961, Saudi Arabia*

* ***Corresponding author:***

email: SSAbdalla@imamu.edu.sa

Received: October 22, 2023
Accepted: January 15, 2024

DOI: 10.22146/ijc.90006

Abstract: *The molecular structure, energetic properties, electronic, and vibrational spectroscopy of meta-substituted phenyl dialumene, DPD (Ar–Al=Al–Ar; Ar of the formula $C_6H_5X_2$, where X = H, CH_3, NH_2, OH, F, Cl, Br, NO_2, and COOH) are investigated by DFT. The singlet states of unsubstituted and substituted DPD adopt trans-planar geometry, while the triplet states adopt non-planar trans-bent geometry. The Al=Al bond length of unsubstituted DPD-H in a singlet state is calculated to be 2.734 Å, and there is no systematic and significant change upon substitution (2.734–2.744 Å). The substitution affects the absolute energy, ionization potential, electron affinity, and reorganization energy. The wavelength of maximum absorbance of DPD-H is determined to be 443 nm, and the substitute analogues DPD-X (X = OH, F, Cl, Br, NO_2, CHO, COOH) show a hypsochromic shift, while DPD-CH_3 and DPD-NH_2 exhibit a bathochromic effect. The HOMO to LUMO+1 transition is the major transition for the meta-substituted DPD, except for X=NO_2, where the transition is to LUMO+2. Considering the reorganization energy values, meta-substituted DPD can be useful as hole transporters. In addition, the theoretical data will aid in predicting the behavior of this class of compounds, facilitating the design and synthesis of similar compounds with desired properties.*

Keywords: *dialumene; DFT; electron affinity; ionization potential; molecular structure; potential energy distribution; reorganization energy*

■ INTRODUCTION

The structure and properties of the homonuclear multiple metal-metal bonded (M=M) compounds that are generally represented as RM=MR (M is a metal element and R is an alkyl or aryl system) have received intensive attention experimentally and theoretically. For instance, Gu and co-workers [1] investigated the Diels–Alder cycloaddition reactions of ArM=MAr with toluene analogous to alkenes theoretically. The preparation, reactivity, and characterization of dimetallenes ($R_2M=MR_2$) and dimetallynes (RM≡MR) of triel (group 13) and tetral (group 14) elements, which are analogues of ethylene and acetylene, respectively, have been reported [2]. Unlike planar ethylene and linear acetylene, dimetallens and dimetallynes have trans-bent structures due to a lack of effective hybridization [3]. Over the years, several studies on the synthesis of multiple bond compounds involving heavier main group elements, including group 13, have been carried out due to their unique structures and properties in comparison to compounds containing triel elements, such as alkenes ($R_2C=CR_2$) and ketones ($R_2C=O$) [4].

Though aluminium is the most prevalent metal in the earth's crust, over the past few decades, homodinuclear

multiple-bonded neutral aluminium compounds, which are aluminium counterparts of alkenes, have been notoriously challenging synthetic targets [5-7]. Generally, the synthetic challenges of the main group of homo-dinuclear multiple-bonded compounds have largely been overcomed through the choice of appropriate supporting and sterically hindered ligands that provide sufficient kinetic stabilization to the binuclear multiple bonds. While prior study documented the synthesis of anionic dialumene compounds [8]. The isolation and characterization of the first and second examples of stable neutral substituted dialumene (Al=Al) compounds of the formula $(CH_3)_3CCH_3Si–Al=Al–SiCH_3C(CH_3)_3$ and Tipp–Al=Al–Tipp (Tipp = 2,4,6-tri-isopropylphenyl) that are stabilized by *N*-heterocyclic carbenes (1,3-di-iso-propyl-4,5-dimethyl-imidazolin-2-ylidene) were reported [6,9].

However, a handful of unsaturated diborene (B=B) and diboryne (B≡B) containing compounds have been reported [10]. In addition, heavier triels neutral compounds Ar–M=M–Ar of gallium, indium and titanium stabilized by sterically aryl groups have been isolated and characterized [11].

The reactions of these unsaturated homo-dinuclear compounds have been extensively studied. For example, these compounds are reported to react readily with olefins, polyolefins, alkynes, and inorganic compounds [12-13]. These compounds are well known for the unique bond activation reactions of small molecules (such as hydrogen, ammonia, carbon monoxide, and carbon dioxide) that were customarily dominated by transition metal compounds [3,9-10,14-15]. In addition, the reactivity, electronic, and structural properties of the neutral double-bonded binuclear compounds of group 13 elements stabilized with bulky ligands have been studied using the density functional theory (DFT) method [15]. The DFT results show that all triel atoms have an M=M double bond character except the heaviest atom, thalium (Tl), which is characterized by a Tl–Tl single bond. The lighter atoms (B, Al, and Ga) adopt an M=M planar configuration, while the heavier atoms (In and Tl) have trans-bent structures, and the MM bond distances increase as the size of the triel atoms (M) increases [15]. The DFT method has also been used to study the effect of substituents on the structural and electronic properties of

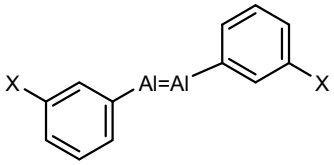

(X=H, CH_3, NH_2, F, Cl, Br, NO_2, CHO, COOH)

Fig 1. Structure of unsubstituted and substituted dialumenes

substituted dialumenes (Ar–M=M–Ar, Ar = para-substituted aryl group) [16]. In this article, we attempted to investigate the structural and electronic properties of diphenyl dialumenes (DPD) of the formula (ArAl=AlAr). Special attention has been paid to the influence of the substitution in the meta positions of the phenyl groups on the molecular structures, frontier orbitals, and electronic and optical properties. Fig. 1 represents the structures of DPD.

■ COMPUTATIONAL METHODS

All calculations were carried out using the DFT-B3LYP along with the 6-311+G(d,p) basis set incorporated in the Gaussian 09 suite program [17]. The electronic properties: the highest occupied molecular orbital (HOMO), the lowest unoccupied molecular orbital (LUMO) energies, the HOMO-LUMO energy gap, the ionization potential (IPs), the electron affinity (EAs), the hole extraction potential (HEP), the electron extraction potential (EEP), the reorganization energy expressed as electron reorganization ($\lambda_{electron}$), and the hole transfer (λ_{hole}) were calculated using the optimized structures [18]. The wavelengths of maximum absorbance (λ_{max}) were also calculated using time-dependent DFT (TD-DFT) [19] using the same hybrid functional and basis set as used for the optimization. The adiabatic electron affinity (EA_A) is given by the difference between the total energy of the neutral molecule $E(G_0^0)$ at its most stable geometry and that of the anionic molecule $E(G_-^-)$ at its most stable conformation (Eq. (1)).

$$EA_A = E\left(G_0^0\right) - E\left(G_-^-\right) \quad (1)$$

The vertical electron affinity (EA_v) is given by the difference between the total energy of the neutral molecule $E(G_0^0)$ at its most stable geometry and that of

Table 1. Geometrical parameters of DPD and its derivatives in singlet and triplet states (Ar–Al=Al–Ar), bond lengths (Å), bond angles, and dihedral angles (°)

X	Singlet				Triplet			
	Bond length		Bond angle	Dihedral angle	Bond length		Bond angle	Dihedral angle
	Al–Al	Al–C	C–Al–Al	C–Al–Al–C	Al–Al	Al–C	C–Al–Al	C–Al–Al–C
H	2.734	1.991	120.4	180.0	2.418	1.970	145.9	169.0
Me	2.734	1.990	120.5	180.0	2.419	1.970	146.0	175.2
NH_2	2.734	1.990	120.8	180.0	2.419	1.970	146.2	174.3
OH	2.740	1.994	120.2	180.0	2.417	1.972	145.8	167.6
F	2.741	1.996	119.8	180.0	2.418	1.973	145.6	176.5
Cl	2.741	1.997	119.7	180.0	2.418	1.974	145.2	166.6
Br	2.744	1.998	119.5	180.0	2.418	1.974	145.2	164.7
NO_2	2.746	2.005	118.9	180.0	2.417	1.976	143.4	175.7
CHO	2.736	1.997	119.8	180.0	2.419	1.974	144.8	175.8
COOH	2.739	1.996	119.7	180.0	2.418	1.973	144.6	176.1

the anion molecule $E(G_0^-)$ at the geometry of the neutral (Eq. (2)).

$$EA_v = E\left(G_0^0\right) - E\left(G_0^-\right) \quad (2)$$

The adiabatic ionization potential (IP_A) is defined as the difference in the total energies of the cation and the neutral species in their most stable geometries. Therefore, IP_A can be determined using the following equation (Eq. (3)):

$$IP_A = E\left(G_+^+\right) - E\left(G_0^0\right) \quad (3)$$

where $E(G_0^0)$ is the total energies of neutral molecules and $E(G_+^+)$ is the energy of cationic molecules. The vertical ionization potential (IP_v) is calculated by subtracting the total energy of the neutral molecules from the energy of the cation molecule obtained at the geometry of neutral molecules (Eq. (4));

$$IP_v = E\left(G_0^+\right) - E\left(G_0^0\right) \quad (4)$$

where $E(G_0^+)$ is the total energies of the cationic state of molecules calculated at the same equilibrium geometry as the neutral molecules [20-21]. The electron reorganization energies ($\lambda_{electron}$) can be expressed in Eq. (5):

$$\lambda_{electron} = EEP - EA_v \quad (5)$$

where electron extraction potential (EEP) is given by Eq. (6):

$$EEP = E\left(G_-^0\right) - E\left(G_-^-\right) \quad (6)$$

where $E(G_-^0)$ and $E(G_-^-)$ are the total energies of the anion and neutral in the ionic geometry, respectively. The hole reorganization energies (λ_{hole}) can be expressed in Eq. (7):

$$\lambda_{hole} = IP_v - HEP \quad (7)$$

The hole extraction potential (HEP) represents the difference in the energy between the cationic in their equilibrium structure $E(G_{0+}^+)$ and the energy of the natural in the cationic geometry (Eq. (8)).

$$HEP = E\left(G_+^+\right) - E\left(G_+^0\right) \quad (8)$$

The Multiwfn program [22] was used for the topological analysis of electron density. The critical points were determined. The density at CP ($\rho(r_c)$) and its Laplacian ($\nabla^2(r_c)$) were calculated at the B3LYP/6-311+G(d,p) level of theory. The potential energy distribution (PED) implemented in the VEDA4 program was used to identify typical vibrational modes in the studied molecules. The VEDA4 program automatically extracts input data from the Gaussian check files and proposes an introductory set of local mode coordinates that are optimized to get the most elements possible from each coordinate in the PED matrix [23-24].

■ RESULTS AND DISCUSSION

Geometrical Analysis

The geometrical analysis of the substituted DPD shows that the singlet state molecules are trans-planar,

with the C–Al–Al–C dihedral angles of about 180° and the C–Al–Al bond angles of nearly 120° typical of sp^2 hybridized systems. On the other hand, the triplet states of the molecules adopt non-planar trans-bent geometry with C–Al–Al bond angles of around 145° and C–Al–Al–C dihedral angles of 167–176°. The DPD-NO_2 has the highest deviation from planarity, having C–Al–Al and C–Al–Al–C bond angles of 143.4 and 175.7°, respectively. Similarly, the electron-withdrawing substituents (–CHO and –COOH) have deviations from planarity as indicated by their bond and dihedral angles (Table 1). The planar geometries for the singlet states and the non-planar geometries for the triplet states are consistent with the previous experimental and theoretical studies [3,15-16]. The Al–Al and Al–C bond distances, C–Al–Al bond angle, and C–Al–Al–C dihedral angle values of substituted DPD in singlet and triplet states are reported in Table 1. The Al–Al bond length of unsubstituted DPD in a singlet state is calculated to be 2.734 Å, and there is no systematic and significant change upon substitution (2.734–2.744 Å). The highest deviation was calculated to be 0.012 Å for the DPD-NO_2. Similarly, the Al–Al bond length in the triplet state, which is calculated to be 2.418 Å for DPD–H, is not significantly affected by substitutions in the *meta*-positions of the phenyl rings (Table 1).

Generally, the Al=Al bond lengths of the triplet states of the molecules are shorter than those of the singlet states, implying that the Al=Al bond in the triplet states has more double character than the singlet states. The double bond character of Al–Al in dialumenes has been supported by both experimental and theoretical studies [5-6,14,16]. Previous studies have reported Al=Al bond length values of 2.394, 2.444, 2.494, 2.420, 2.390, 2.450, and 2.600 Å for different dialumene compounds [5,14,25]. Theoretical values in the ranges of 2.698–2.746 Å and 2.419–2.426 Å have been reported for the singlet and triplet states of para-substituted dialumenes [16]. Upon reaction, the dialumene compounds lose their double bond character to form an elongated Al-Al single bond in the range of 2.53–2.75 Å typical of a single bond having Al–Al bond lengths [5-6,15]. Based on this, the Al–Al bonds in our studied compounds are single bonds in the singlet state and have the double bond character in the triplet state.

The impact of the substitution by electron-withdrawing substituents (F, Cl, Br, NO_2, CHO, and COOH) reveals that the Al=Al and Al–C bonds in singlet states are relatively longer compared to the structures with electron-donating groups. Thus, the electron-donating substituents stabilize the Al–Al and Al–C bonds in the singlet state. The CAlAl bond angles in the singlet states of the molecules are changing due to the presence of the substituent in the meta-positions of the phenyl rings. In general, the CAlAl bond angles increase in the structure with donor substituents and decrease in the structures with electron-withdrawing substituents. In the triplet state, the CAlAl bond angles slightly increase as a result of electron-donating substituent, the highest value is obtained for NH_2 substituent and is calculated to be 146.2°. The electron-withdrawing substituents decrease the CAlAl bond angles. These results conform with the previous study for the para-substituted dialumenes [16].

Singlet-Triplet Energy Gap

The singlet states of unsubstituted and substituted DPD are found to be energetically favored over the singlet states with an energy difference range of 11.10–11.97 kcal/mol. Similar trends were reported for the para-substituted molecules, where their energy difference was reported to be in the range of 10.26–12.00 kcal/mol [16]. For the halogenated DPD, the energy of the molecules decreases with the increase in the size of the halogen atoms (F, Cl, and Br). Table 2 summarizes the total energies of singlet and triplet states as well as the relative energies.

Due to the use of incomplete basis sets for the individual fragments, Basis Set Superposition Error (BSSE) may artificially stabilize the system and lead to an overestimation of the actual interaction energies [17,26]. This effect can be significant even for modest basis sets like 6-311+G(d,p) and needs to be taken into account for accurate quantitative comparisons. In addition, Relativistic the presence of Al atoms in the studied systems introduces relativistic effects that influence the electronic

Table 2. Total energies (in Hartree) of meta-substituted DPD molecules in singlet ($E_{singlet}$) and triplet ($E_{triplet}$) states and their energy difference (ΔE (kcal/mol) = $E_{triplet}$ - $E_{singlet}$)

Substituent (X)	$E_{(singlet)}$	$E_{(triplet)}$	ΔE
H	−948.274772	−948.256704	11.34
Me	−1026.929874	−1026.912092	11.16
NH_2	−1059.027457	−1059.009768	11.10
OH	−1098.769742	−1098.751615	11.37
F	−1146.813447	−1146.794917	11.63
Cl	−1867.522000	−1867.503260	11.76
Br	−6095.361545	−6095.342738	11.80
NO_2	−1357.402356	−1357.383276	11.97
CHO	−1174.990701	−1174.972149	11.64
COOH	−1325.548879	−1325.530286	11.67

structure and energy levels. Neglecting relativistic corrections can lead to deviations in the calculated interaction energies compared to a non-relativistic treatment. The impact of relativistic effects is particularly pronounced for heavier elements like Al [27]. Despite these limitations, the reported energies can still provide valuable insights into the relative energetics of the studied systems and offer a qualitative understanding of the underlying interactions. However, it is crucial to acknowledge these limitations when interpreting and comparing the calculated data with experimental values or theoretical results obtained using more sophisticated methods that include dispersion corrections, BSSE corrections, and relativistic corrections.

Frontier Molecular Orbitals

The frontier orbitals (HOMO and LUMO) are crucial for forecasting the stability and reactivity of molecules [28]. The electron-donating ability of the molecule is represented by the E_{HOMO}, whereas the electron-accepting ability is represented by the E_{LUMO}. Hence, a good electron carrier is one with a higher E_{HOMO} value, whereas a good hole carrier is one with a lower E_{LUMO} value. The reorganization energies of the molecules are thus related to the HOMO and LUMO energies [29]. The HOMO-LUMO gap (ΔE_{gap}) is the energy differential between the HOMO and LUMO. The optical and electrical characteristics of molecules are directly related to the ΔE_{gap} values. The frontier molecular orbital energies of the studied dialumenes, along with their ΔE_{gap} values, are illustrated in Fig. 2.

An inspection of Fig. 2 shows that the substitution increases the values of E_{HOMO} and decreases the values of E_{LUMO}, thereby reducing the ΔE_{gap} from 6.59 eV for DPD

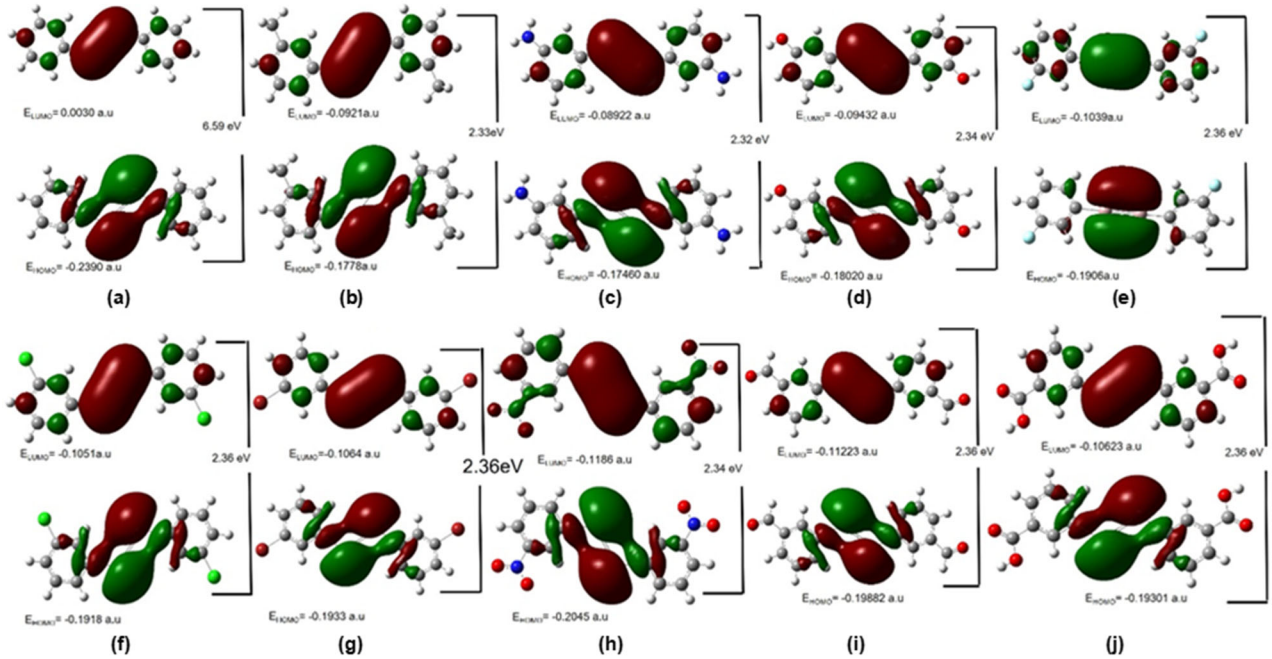

Fig 2. Frontier molecular orbital energies (in Hartree) and energy gap, ΔE_{gap} (in eV) of (a) DPD-H (b) DPD-CH_3(c) DPD-NH_2 (d) DPD-OH (e) DPD-F (f) DPD-Cl (g) DPD-Br (h) DPD-NO_2 (i) DPD-COH and (j) DPD-COOH

to an average value of 2.35 eV (about a 64% reduction upon substitution) for the substituted DPD compounds. The electron-donating substituents decrease the ΔE_{gap} values more than the electron-donating substituents (2.34–2.36 eV). The overall effect of substitution appears to be a decrease in the HOMO-LUMO gap upon substitution. These findings for meta-substitution DPD are similar to the previous studies on para-substituted dialumenes [16]. In addition, Fig. 2 clearly shows that both HOMO and LUMO are essentially localized on the Al–Al π-bond between the two aluminium atoms. These frontier energy values are consistent with the HOMO-LUMO energy gap value of 2.24 eV reported for a neutral dialumene compound stabilized with bulky ligands [6].

Ionization Potential (IP), Electron Affinity (EA), and Reorganization Energies (λ_{hole} and $\lambda_{electron}$)

The EA and IP are very important molecular descriptors that are related to the reactivity of molecules. The electron affinity reflects the ability of a molecule to gain electrons and the ionization potential reflects the ability of the molecule to lose an electron. Consequently, the ionization potential is associated with the potentiality of the molecule to form a hole. On the contrary, electron affinity is associated with the ability of the molecule to carry an additional electron. The greater the electron affinity, the weaker the ability of the molecule to gain electrons. Based on the molecular descriptors, one can justify the connection between the molecular structure and electronic behavior. The B3LYP/6-311+G(d,p) level of theory is implemented to calculate the electron affinity and the ionization potential in addition to the reorganization energies (λ_{hole} and $\lambda_{electron}$).

Table 3 reports the electron affinity and ionization potential (adiabatic and vertical) as well as the hole (λ_{hole}) and electron ($\lambda_{electron}$) reorganizations for meta-substituted DPD. The values of the EA and IP increase with the substitution by the electron-withdrawing groups. In contrast, the electron-donating substituents cause a decrease in the EA and IP values. The IP_A values increase with electron-withdrawing groups. The IP_v also increases from donor groups to electron-withdrawing groups (IP_v = 6.32 eV for DPD-NH_2 to IP_v = 7.22 eV for DPD-NO_2). On the other hand, the lowest EA_a among donor electron groups is observed for DPD-NH_2 (1.04 eV) and the largest electron affinity is for DPD-NO_2 (2.42 eV). The NO_2 substitution increases the hole reorganization energy (λ_{hole}), which can be attributed to the higher electron-withdrawing effect of the nitro group [29]. NH_2-substitution has lower EA and IP values and the highest value of λ_{hole}. These results are observed to be similar to the para-substituted dialumenes [16].

Among the electron-donating groups, the substitution with the methyl function possesses the highest EA and IP and the lowest $\lambda_{electron}$. It has been determined that the internal reorganization energy ($\lambda_{hole/electron}$) of the electron and hole is mostly responsible for the mobility of charges. The reorganization of energy values gives insight into the variations in the total energies when the structure of the molecules is changed from neutral to charged ones (Eq. (5, 7)). Nevertheless, it sounds feasible that high reorganization energy values

Table 3. EA_A, EA_v, IP_A, IP_v, HEP, EEP, and reorganization energy (λ_{hole}, $\lambda_{electron}$) for substituted DPD (ArAl=AlAr) molecules (eV)

Substituent	EA_A	EA_v	IP_A	IP_v	HEP	EEP	λ_{hole}	$\lambda_{electron}$
H	1.37	1.22	6.19	6.33	5.78	1.38	0.55	0.16
NH_2	1.04	0.89	5.62	6.32	5.20	1.15	1.12	0.26
OH	1.22	1.13	5.86	6.54	6.19	1.41	0.35	0.28
CH_3	1.22	1.13	5.99	6.31	5.62	1.32	0.69	0.19
F	1.58	1.38	6.35	6.67	5.96	1.63	0.71	0.25
Cl	1.59	1.49	6.36	6.70	5.97	1.67	0.73	0.18
Br	1.63	1.53	6.37	6.69	5.97	1.73	0.72	0.20
NO_2	2.42	2.32	6.87	7.22	6.49	2.52	0.73	0.20
CHO	1.83	1.73	6.59	6.92	6.19	1.93	0.73	0.20
COOH	1.66	1.56	6.43	6.77	6.03	1.77	0.74	0.21

correspond to significant structural changes following electron addition and subtraction. According to the data gathered in Table 3, the electron transfer rates are lower than the hole transfer rates since all λ_{hole} values are greater than their corresponding $\lambda_{electron}$ values. These results are analogous to the para-substituted DPD [16]. These findings suggest that the studied compounds could be used as hole electron transporters, and to attain this, further research is essential.

Electronic Spectra

The UV-vis electronic properties of DPD and their derivatives were calculated using the TD-DFT [19]. The maximum wavelength of absorbance (λ_{max}), oscillator strength (η), excitation energy, assignment of the transition and percentage molecular orbital contribution associated with λ_{max} are provided in Table 4. Fig. 3 illustrates the simulated UV-absorption spectra of unsubstituted DPD-H and its substituted derivatives (DPD-X) of dialumenes. The DPD-H has λ_{max} at 443 nm that is attributed to HOMO to LUMO+1 transition with a percentage molecular orbital contribution of about 99%. Upon substitution, the shift of the absorption spectral band to a shorter wavelength is observed for all the substituted DPD-X (X = OH, F, Cl, Br, NO_2, CHO, COOH) except DPD-CH_3 and DPD-NH_2, which exhibited bathochromic effect with λ_{max} values of 445 and 447 nm respectively.

Though the carbonyl groups of DPD-CHO and DPD-COOH are conjugated with the aromatic phenyl rings, both molecules exhibit a hypsochromic effect. Fig. 3 shows the relative positions of the absorption spectral bands of the molecules. The most probable electronic transition in all molecules is associated with the HOMO to LUMO+1 transition, except in DPD-NO_2, where the transition is attributed to HOMO → LUMO+2. This may be attributed to the fact that the NO_2 functional group has two heteroatoms, each of which has an unpaired electron, and the molecular orbital analysis provides that HOMOs and LUMO+1 are of the σ characteristics, but LUMOs and LUMO+2 are of the π characteristics. These results are consistent with previous calculations for the para-substituted dialumenes [16]. In addition, these transitions are mostly pure transitions with a percentage molecular orbital contribution of about 99%. The B3LYP functional employed in this study does not explicitly account for dispersion interactions, which play a crucial role in stabilizing non-covalent interactions. This omission can lead to inaccurate results for systems involving significant dispersion interactions, such as those studied here. Moreover, B3LYP underestimates the HOMO-LUMO gap, which can lead to an overestimation of the calculated absorption wavelength. Despite this limitation, B3LYP remains a versatile and powerful DFT method applicable to a wide range of chemical systems [30-31].

Table 4. Maximum absorption wavelength (λ_{max}), excitation energy (eV), and oscillator strength (η) for substituted dialumenes

Substituent	λ_{max} (nm)	E (eV)	η	Assignment*
H	443	2.80	0.4448	H→L+1 (99%)
CH_3	445	2.79	0.4596	H→L+1 (99%)
NH_2	447	2.78	0.4623	H→L+1 (98%)
OH	439	2.82	0.4536	H→L+1 (99%)
F	436	2.85	0.4566	H→L+1 (99%)
Cl	439	2.84	0.4768	H→L+1 (99%)
Br	438	2.83	0.4915	H→L+1 (99%)
NO_2	434	2.86	0.4219	H→L+2 (99%)
COH	438	2.83	0.4807	H→L+1 (99%)
COOH	436	2.84	0.4817	H→L+1 (99%)

*H = HOMO and L = LUMO

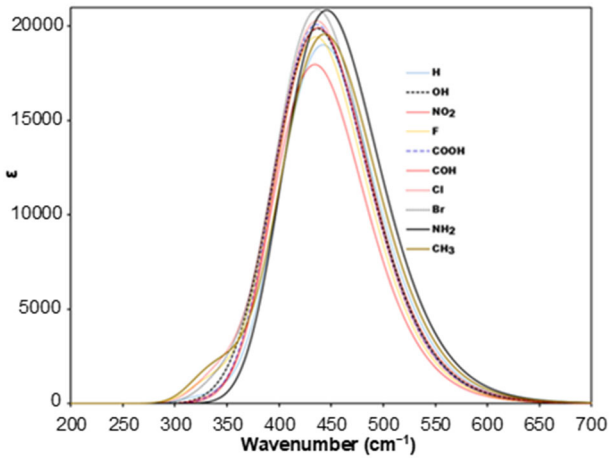

Fig 3. Simulated UV spectra of DPD and its derivatives

Molecular Electrostatic Potential (MEP)

The study of MEP is indispensable to understanding and predicting the relationship between the molecular structure and the molecular interaction

[32]. The visual method of MEP is used to distinguish the location of the electron density and charge distribution within the molecule. The information on the charge distributions can be used to determine how molecules interact with one another. The GaussView [33] is used to map the MEP onto the molecular surface by using the optimized structures. The 2D plots of the molecular electrostatic potential of DPD and its derivatives are shown in Fig. 4. In this particular case, the colors have been chosen such that regions of attractive potential appear in red or yellow and are associated with electrophilic reactivity and represent the negative potential of MEP, while those of repulsive potential appear in blue and are associated with nucleophilic reactivity and represent the positive potential of MEP, thus being the suitable center of the electrophilic attacks.

Quantum Theory of Atoms in Molecules (QTAIMs) Analysis

The QTAIM is a distinctive conception of chemical bonding. QTAIM defines bonding by using a topological analysis of the electron density distribution [34-35]. The bond identified by the analysis is assumed to be an indicator of a special pair-wise physical relationship between atoms. Application of QTAIM allows us to find bond critical points (BCP) and analyze their properties, including electron density ($\rho(r_{cp})$) and the Laplacian of electron density ($\nabla^2\rho\ (r_{cp})$) at the bond critical point r_{cp}.

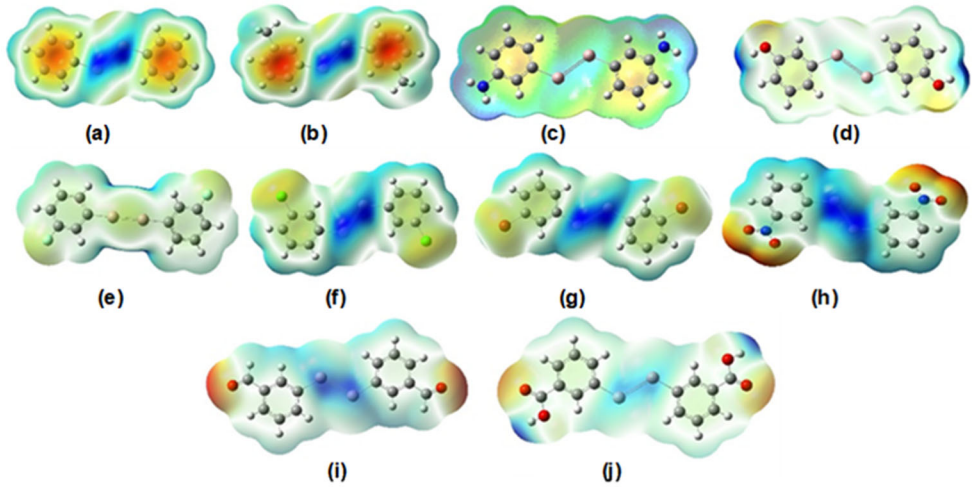

Fig 4. 2D map of the molecular electrostatic potential of DPD and its derivatives (a-i) (a) DPD (b) DPD-CH_3 (c) DPD-NH_2 (d) DPD -OH (e) DPD-F (f) DPD-Cl (g) DPD-Br (h) DPD-NO_2, and (i) DPD-COOH

Table 5. Electron densities ($\rho(r_{cp})$), Laplacians ($\nabla^2\rho(r_{cp})$), kinetic energy density K(ρ), potential energy density V(ρ), and total electron energy density H(ρ) at Al–Al and Al–C critical points for DPD and its derivatives. All properties are calculated (a.u.)

	Al–Al					Al–C				
X	ρ(rcp)	$\nabla^2\rho$(rcp)	K(ρ)	V(ρ)	H(ρ)	$\rho(r_{cp})$	$\nabla^2\rho(r_{cp})$	K(ρ)	V(ρ)	H(ρ)
H	0.04101	−0.03775	0.00372	−0.01674	−0.01302	0.08061	0.28541	0.09553	−0.11754	−0.02201
CH_3	0.03879	−0.03272	0.00362	−0.01543	−0.01181	0.08040	0.28321	0.09313	−0.11620	−0.02307
NH_2	0.03887	−0.03385	0.00359	−0.01575	−0.01216	0.08012	0.29390	0.09648	−0.11945	−0.02297
OH	0.03856	−0.03321	0.00358	−0.01556	−0.01198	0.08156	0.28743	0.09504	−0.11786	−0.02282
F	0.03852	−0.03265	0.00363	−0.01543	−0.01180	0.07990	0.28121	0.09310	−0.11580	−0.02270
Cl	0.03884	−0.03258	0.00359	−0.01536	−0.01177	0.07955	0.27856	0.09240	−0.11510	−0.02270
Br	0.03878	−0.03254	0.00358	−0.01534	−0.01176	0.07950	0.27778	0.09215	−0.11490	−0.02275
NO_2	0.03836	−0.03138	0.00357	−0.01503	−0.01146	0.07822	0.26680	0.08907	−0.11135	−0.02228
COH	0.03855	−0.03179	0.00361	−0.01511	−0.01150	0.07870	0.27031	0.09017	−0.11280	−0.02263
COOH	0.03860	−0.03188	0.00361	−0.01516	−0.01155	0.07897	0.27158	0.09067	−0.11323	−0.02256

The kinetic energy density K(ρ), potential energy density V(ρ), and total electron energy density H(ρ) at the critical points are also computed. Table 5 presents the results of the topological analysis of the critical points of Al–Al and Al–C bonds for the most stable species. The values of $\rho(r_{cp})$ and their corresponding $\nabla^2\rho(r_{cp})$ calculated at the BCP of a given bond agree with the strength and length of these bonds.

The total energy density is obtained from the equation H(ρ) = K(ρ) + V(ρ), where K(ρ) and V(ρ) are the local kinetic densities, positive, and potential energy densities, negative, respectively [34]. Based on the quantum theory of atoms in molecules, the large values of ρ(r) and the negative values of $\nabla^2\rho(r_{cp})$ and H(r) indicate shared electron interactions (i.e., covalent bonds), while the small values of ρ(r) and the positive values of $\nabla^2\rho(r_{cp})$ and H(ρ) indicate stable bonding and pure closed-shell interactions (ionic, hydrogen bonds, and van der Waals interactions) [34]. The density values at the BCP of Al–Al bonds are positive, and their corresponding $\nabla^2\rho(r_{cp})$ suggest that electron density is concentrated around the bond critical point (BCP) of the Al–Al bonds as long as all $\nabla^2\rho(r_{cp})$ values are negative. These values are consistent with shared interaction (covalent bond) and agree with the recent topological study of the double bond nature of the Al=Al bond [36].On the other hand, the density values at the BCP of Al–C are positive, and the corresponding values of $\nabla^2\rho(r_{cp})$ are positive, suggesting that the Al–C bonds are a close shell interaction of an ionic character. However, the total energy density H(ρ) at a BCP is considered a reliable index to characterize the weak interaction compared with $\nabla^2\rho(r_{cp})$ [37]. Thus, the negative values of the H(ρ) suggest that the potential energy overcomes the kinetic energy densities and the Al–C bonds have a share interaction, i.e., covalent character.

Vibrational Energy Distribution Analysis

In the present study, the vibrational wavenumbers and their relative intensities were calculated, and assignments of the vibrational modes were proposed using the potential energy distributions (PED) as implemented in the VEDA 4 program [23]. The simulated vibrational spectra (3500–500 cm^{-1}) of the studied DPD molecules are presented in Fig. 5. This figure shows characteristic vibrational peaks that are typical of the functional groups in the molecules. All the molecules show a vibrational peak around 3,200 cm^{-1}, which are characteristics of CH symmetric and asymmetric vibrational modes. These are all pure CH modes with percentage contributions of about 85–98% to PED. Since the Al–Al bond is the main feature of the DPD, the Al–Al and Al–C stretching modes are presented in Table 6, along with their intensities and contributions to PED. These modes appeared in the fingerprint region of the vibrational spectra of the molecules (Fig. 5).

The Al–Al stretching mode of unsubstituted DPD which is calculated to be at 256 cm^{-1} was found to be at

Table 6. Calculated vibrational parameters of stretching of Al–Al and Al–C bonds for DPD and its derivatives computed at the B3LYP/6-311+G(d,p) level of theory

Substituents	Wavenumber (cm^{-1})	IR intensity (km/mol)	Assignment* (PED ≥ 10%)
H	683	0.00	νAlC(20)
	681	36.92	νAlC(19)
	380	0.01	νAlC(53) + νAlAl(13)
	351	132.27	νAlC(66)
	256	0.00	νAlAl(30)
	125	0.00	νAlAl(56)
CH_3	683	0.00	νAlC(10)
	681	27.26	νAlC(11)
	380	0.03	νAlC(50)
	361	55.10	νAlC(23)
	342	94.30	νAlC(42)
	244	0.00	νAlAl(43)
	100	0.10	νAlAl(46)

Substituents	Wavenumber (cm^{-1})	IR intensity (km/mol)	Assignment* (PED ≥ 10%)
NH_2	372	9.23	νAlC(40)
	345	135.00	νAlC(59)
	243	0.03	νAlAl(36)
	109	1.06	νAlAl(48)
OH	681	0.00	νAlC(15)
	679	43.13	νAlC(20)
	341	127.40	νAlC(67)
	243	0.00	νAlAl(24)
	119	0.00	νAlAl(58)
F	365	0.00	νAlC(23) + υAlAl(14)
	339	119.20	νAlC(30)
	243	0.00	νAlAl(30)
	119	0.00	νAlAl(54)
Cl	370	0.00	νAlC(19)
	348	116.60	νAlC(23)
	318	0.00	νAlAl(10)
	228	0.00	νAlAl(27)
	116	0.00	νAlAl(52)
Br	729	0.01	νAlC(17)
	728	41.10	νAlC(15)
	376	0.00	νAlC(51)+ νAlAl(11)
	355	92.60	νAlC(56)
	223	0.00	νAlAl(49)
	64	0.00	νAlC(11) + νAlAl(36)
CHO	712	0.00	νAlC(11)
	375	0.00	νAlC(53)
	374	0.00	νAlAl(10)
	340	163.00	νAlC(66)
	267	0.00	νAlAl(14)
	214	0.00	νAlAl(29)
	88	0.00	νAlC(15) + νAlAl(47)
COOH	921	0.00	νAlC(11)
	824	0.00	νAlC(29)
	820	0.00	νAlC(14)
	594	0.00	νAlC(41)
	594	0.00	νAlC(10)
	593	0.00	νAlC(11)
	405	0.00	νAlAl(71)

*ν is stretching

lower wavenumber 244 cm^{-1} (DPD-CH_3) 243 cm^{-1} (DPD-NH_2, DPD-OH and DPD-F), 220 cm^{-1} (DPD-NO_2), 228 cm^{-1} (DPD-Cl), 223 cm^{-1} (DPD-Br), and a longer vibrational wavenumber of 267 cm^{-1} (DPD-CHO) and 405 cm^{-1} (DPD-COOH). In addition, DPD-CHO shows strong peaks at around 1,766 and 1,767 cm^{-1} that is attributed to the symmetric and asymmetric CO with PED values of 89%. The CO stretching modes for the DPD-COOH appeared at a longer wavelength of 1,783/1,784 cm^{-1}, and the peak at 3,772 cm^{-1} are attributed to the OH stretching of the molecule. The OH vibrational mode of DPD-OH is calculated to be at 3,832 cm^{-1}. For DPD-NH_2, the asymmetric and symmetric NH stretching modes are calculated to be at 3,662/3,663 and 3,565/3,566 cm^{-1} respectively. We are acknowledging the current absence of directly comparable experimental or theoretical FTIR data for validation. Nevertheless, our simulated FTIR results are reliable.

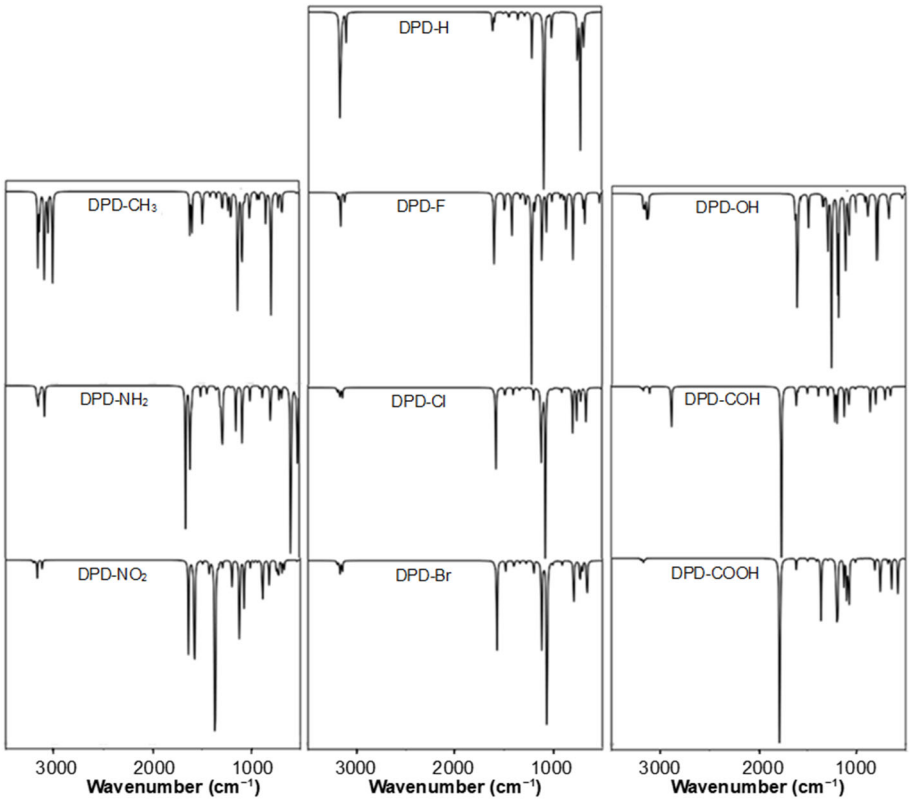

Fig 5. Simulated IR spectra of DPD and its derivatives computed at the B3LYP/6-311+G(d,p) level of theory

■ CONCLUSION

The molecular structure, electronic properties, reorganization energies, molecular electrostatic potential, topology analysis of atoms in a molecule, and vibrational spectra of DPD and its derivatives are computed by using DFT and with the aid of 6-311+G(d,p). The results show the geometry of the singlet states of the molecules are trans-planar, with the C–Al–Al–C dihedral angles of about 180° and the C–Al–Al bond angles of nearly 120° typical of sp^2 hybridized systems. On the other hand, the triplet states of the molecules adopt non-planar trans-bent geometry with C–Al–Al bond angles of around 145°. Substitution has a significant influence on the total energy of the molecules, with DPD-Br having the lowest energy. According to the values of the reorganization energy, the substituted DPD can be applied as hole transporters. The most intense electronic transition in all the molecules is associated with the HOMO → LUMO+1 transition except in NO_2 substitution, which is associated with HOMO → LUMO+2, and may be attributed to the fact that the NO_2 functional group has two types of heteroatoms. In addition, substitutions lead to both bathochromic and hypsochromic spectral shifts depending on the nature of the substituent. The QTAIMs analysis reveals that the Al–Al bond has a shared interaction character, while the Al–C bond has an ionic character. The Al–Al vibrational modes of the molecules are calculated to be in the fingerprint regions of the vibrational IR spectra of the molecules.

■ CONFLICT OF INTEREST

The authors declare no conflicts of interest.

■ AUTHOR CONTRIBUTIONS

Salma Babikir and Wefag Mohamed performed the DFT calculations and drafted the manuscript. Sahar Abdalla performed the QTAIM analysis. Sahar Abdalla and Yunusa Umar wrote and revised the manuscript. All authors approved the final version of the manuscript.

■ REFERENCES

[1] Gu, S.Y., Sheu, J.H., and Su, M.D., 2007, Theoretical studies of the [2 + 4] Diels–Alder cycloaddition

reactions of alkene analogues of the group 13 elements with toluene, *Inorg. Chem*., 46 (6), 2028–2034.

[2] Rivard, E., and Power, P.P., 2007, Multiple bonding in heavier element compounds stabilized by bulky terphenyl ligands, *Inorg. Chem.*, 46 (24), 10047–10064.

[3] Hanusch, F., Groll, L., and Inoue, S., 2020, Recent advances of group 14 dimetallenes and dimetallynes in bond activation and catalysis, *Chem. Sci.*, 12 (6), 2001–2015.

[4] Mizuhata, Y., Sasamori, T., and Tokitoh, N., 2009, Stable heavier carbene analogues, *Chem. Rev*., 109 (8) 3479–3511.

[5] Bag, P., Weetman, C., and Inoue, S., 2018, Experimental realisation of elusive multiple-bonded aluminium compounds: A new horizon in the aluminium chemistry, *Angew. Chem. Int. Ed.*, 57 (44) 14394–14413.

[6] Bag, P., Porzelt, A., Altmann, P.J., and Inoue, S., 2017, A stable, neutral compound with an aluminium–aluminium double bond, *J. Am. Chem. Soc*., 139 (41), 14384–14387.

[7] Hobson, K., Carmalt, C.J., and Bakewell, C., 2020, Recent advances in low oxidation state aluminium chemistry, *Chem. Sci.*, 11 (27), 6942–6956.

[8] Wright, R.J., Brynda, M., and Power, P.P., 2006, Synthesis and structure of the "dialuminyne" $Na_2[Ar'AlAlAr']$ and $Na_2[(Ar''Al)_3]$: Al-Al bonding in Al_2Na_2 and Al_3Na_2 clusters, *Angew. Chem. Int. Ed.*, 45 (36), 5953–5956.

[9] Weetman, C., Porzelt, A., Bag, P., Hanusch, F., and Inoue, S., 2020, Dialumenes – aryl vs. silyl stabilisation for small molecule activation and catalysis, *Chem. Sci.*, 11 (18), 4817–4827.

[10] Arrowsmith, M., Braunschweig, H., and Stennett, T.E., 2017, Formation and reactivity of electron-precise B–B single and multiple bonds, *Angew. Chem. Int. Ed.*, 56 (1), 96–115.

[11] Weetman, C., 2021, Main group multiple bonds for bond activations and catalysis, *Chem. - Eur. J.*, 27 (6), 1941–1954.

[12] Sugahara, T., Guo, J.D., Sasamori, T., Nagase, S., and Tokitoh, N., 2018, Regioselective cyclotrimerization of terminal alkynes using a digermyne, *Angew. Chem. Int. Ed.*, 57 (13), 3499–3503.

[13] Zhao, Y., Lei, Y., Dong, Q., Wu, B., and Yang, X.J., 2013, Reactivity of dialumane and "dialumene" compounds toward alkenes, *Chem. Eur. J.*, 19 (36), 12059–12066.

[14] Weetman, C., Bag, P., Szilvási, T., Jandl, C., and Inoue, S., 2019, CO_2 Fixation and catalytic reduction by a neutral aluminium double bond, *Angew. Chem. Int. Ed.*, 58 (32), 10961–10965.

[15] Yanga, M.C., and Su, M.D., 2019, Theoretical investigations of the reactivity of neutral molecules that feature an M=M (M = B, Al, Ga, In, and Tl) double bond, *New J. Chem.*, 43 (24), 9364–9375.

[16] Ghiasi, R., and Heidarbeigi, A., 2016, Substituent effect on the structure and properties of dialumene, *Russ. J. Inorg. Chem.*, 61 (8), 985–992.

[17] Frisch, M.J., Trucks, G.W., Schlegel, H.B., Scuseria, G.E., Robb, M.A., Cheeseman, J.R., Scalmani, G., Barone, V., Mennucci, B., Petersson, G.A., Nakatsuji, H., Caricato, M., Li, X., Hratchian, H.P., Izmaylov, A.F., Bloino, J., Zheng, G., Sonnenberg, J.L., Hada, M., Ehara, M., Toyota, K., Fukuda, R., Hasegawa, J., Ishida, M., Nakajima, T., Honda, Y., Kitao, O., Nakai, H., Vreven, T., Montgomery, J.A., Jr., Peralta, J.E., Ogliaro, F., Bearpark, M., Heyd, J.J., Brothers, E., Kudin, K.N., Staroverov, V.N., Kobayashi, R., Normand, J., Raghavachari, K., Rendell, A., Burant, J.C., Iyengar, S.S., Tomasi, J., Cossi, M., Rega, N., Millam, J.M., Klene, M., Knox, J.E., Cross, J.B., Bakken, V., Adamo, C., Jaramillo, J., Gomperts, R., Stratmann, R.E., Yazyev, O., Austin, A.J., Cammi, R., Pomelli, C., Ochterski, J.W., Martin, R.L., Morokuma, K., Zakrzewski, V.G., Voth, G.A., Salvador, P., Dannenberg, J.J., Dapprich, S., Daniels, A.D., Farkas, Ö., Foresman, J.B., Ortiz, J.V., Cioslowski, J., and Fox, D.J., 2009, *Gaussian-09 Revision E.01*, Gaussian, Inc., Wallingford, CT.

[18] Petrushenko, I.K., 2015, DFT study on adiabatic and vertical ionization potentials of graphene sheets, *Adv. Mater. Sci. Eng.*, 2015, 262513.

[19] Umar, Y., 2022, Analysis of the structures, electronic and spectroscopic properties of piperidine based analgesic drugs carfentanil and acetylfentanyl, *Arabian J. Sci. Eng.*, 47 (1), 511–522.

[20] Ali, Z., Abdalla, S., Hassan, E.A., Umar, Y., and Al-Mogren, M.M., 2022, Theoretical study of electronic and optical properties of functionalized Indigo and Alizarin as potential organic semi-conductors for solar cells applications, *Mater. Today Commun.*, 32, 104048.

[21] Ali, Z., Abdalla, S., Hassan, E.A., Umar, Y., Al-and Mogren, M.M., 2022, A DFT and TD-DFT study on emodin and purpurin and their functionalized molecules to produce promising organic semiconductor materials, *J. King Saud Univ., Sci.*, 34 (5), 102117.

[22] Lu, T., and Chen, F., 2012, Multiwfn: A multifunctional wavefunction analyzer, *J. Comput. Chem.*, 33 (5), 580–592.

[23] Jamróz, M.H., 2013, Vibrational energy distribution analysis (VEDA): Scopes and limitations, *Spectrochim. Acta, Part A*, 114, 220–230.

[24] Abdalla, S., Umar, Y., and Mokhtar, I., 2016, Conformational and vibrational analysis of 2-, 3- and 4-pyridinecarbonyl chloride using DFT, *Z. Phys. Chem.*, 230 (5-7), 867–882.

[25] Falconer, R.L., Byrne, K.M., Nichol, G.S., Krämer, T., and Cowley, M.J., 2021, Reversible dissociation of a dialumene, *Angew. Chem. Int. Ed.*, 60 (46), 24702–24708.

[26] Vidal Vidal, A., de Vicente Poutás, L.C., Nieto Faza, O., and Silva López, C., 2019, On the use of popular basis sets: Impact of the intramolecular basis set superposition error, *Molecules*, 24 (20), 3810.

[27] Nakajima, T., and Hirao, K., 2005, Recent development of relativistic molecular theory, *Monatsh. Chem.*, 136 (6), 965–986.

[28] Umar, Y., Abdalla, S., Haque, S.M., Moran, G.S., Ishaq, A., Villada, W.C., Leone, J.D., and Bunster, M., 2020, Theoretical investigation of the molecular structure, vibrational spectra, and molecular docking of tramadol using density functional theory, *J. Chin. Chem. Soc.*, 67 (1), 62–71.

[29] Oshi, R., Abdalla, S., and Springborg, M., 2017, Study of the influence of functionalization on the reorganization energy of naphthalene using DFT, *Comput. Theor. Chem.*, 1099, 209–215.

[30] Grimme, S., Hansen, A., Brandenburg, J.G., and Bannwarth, C., 2016, Dispersion-corrected mean-field electronic structure methods, *Chem. Rev.*, 116 (9), 5105–5154.

[31] Mardirossian, N., and Head-Gordon, M., 2017, Thirty years of density functional theory in computational chemistry: An overview and extensive assessment of 200 density functionals, *Mol. Phys.*, 115 (19), 2315–2372.

[32] Murray, J.S., and Politzer, P., 2017, Molecular electrostatic potentials and noncovalent interactions, *WIREs Comput. Mol. Sci.*, 7 (6), e1326.

[33] Dennington, R., Keith, T.A., and Millam, J.M., 2016, *GaussView, Version 6*, Semichem Inc., Shawnee Mission, KS.

[34] Bader, R.F.W., and Fang, D.C., 2005, Properties of atoms in molecules: Caged atoms and the Ehrenfest force, *J. Chem. Theor. Comput.*, 1 (3), 403–414.

[35] Esser, S., 2019, The quantum theory of atoms in molecules and the interactive conception of chemical bonding, *Philos. Sci.*, 86 (5), 1307–1317.

[36] Michalski, M., Gordon, A.J., and Berski, S., 2019, The nature of the T=T double bond (T=B, Al, Ga, In) in dialumene and its derivatives: Topological study of the electron localization function (ELF), *J. Mol. Model.*, 25 (8), 211.

[37] Dorosti, N., Nikpour, S., Molaei, F., and Kubicki, M., 2021, A triorganotin(IV) cocrystal with pyridinic phosphoramide: Crystal structure and DFT calculations, *Chem. Pap.*, 75 (6), 2503–2516.